



HAL
open science

A MODEL FOR MICRO THREAD MILLING OPERATION (MTMO)

Anna Carla Araujo, Jose Luis Lopes Silveira

► **To cite this version:**

Anna Carla Araujo, Jose Luis Lopes Silveira. A MODEL FOR MICRO THREAD MILLING OPERATION (MTMO). The Canadian Society for Mechanical Engineering Forum 2010, 2010, Victoria, Canada. hal-03212850

HAL Id: hal-03212850

<https://hal.science/hal-03212850>

Submitted on 30 Apr 2021

HAL is a multi-disciplinary open access archive for the deposit and dissemination of scientific research documents, whether they are published or not. The documents may come from teaching and research institutions in France or abroad, or from public or private research centers.

L'archive ouverte pluridisciplinaire **HAL**, est destinée au dépôt et à la diffusion de documents scientifiques de niveau recherche, publiés ou non, émanant des établissements d'enseignement et de recherche français ou étrangers, des laboratoires publics ou privés.

A MODEL FOR MICRO THREAD MILLING OPERATION (MTMO)

Anna Carla Araujo
Department of Mechanical Engineering
POLI - Federal University of Rio de Janeiro
Rio de Janeiro, Brazil
anna@mecanica.ufrj.br

Jose Luis Lopes da Silveira
Department of Mechanical Engineering
COPPE and POLI - Federal University of Rio de Janeiro
Rio de Janeiro, Brazil
jluis@mecanica.ufrj.br

Abstract— The machining of miniaturized components is now a days one of the most important fields of interest in manufacturing and a new tool similar to thread milling is appearing in the market to produce micro threads. This paper investigates a thread making process in micro scale, called micro thread milling operation (MTMO) and presents a new model. The model assumes that the feed direction is linear neglecting the axial feed, which is reasonable for low rates. A chip thickness and mechanistic cutting force model is developed for a thread milling operation with a micro milling tool. As the depth-of-cut to tool diameter ratio is much higher in micro thread milling than the conventional one, the chip thickness is calculated considering the trajectory of the tool tip while the tool rotates and moves continually. Micro milling specific cutting pressure is used as calibration. Numerical results for two different commercial tool dimensions are presented and tool run-out is included.

Keywords- Force prediction; Thread milling; Micromanufacturing.

I. INTRODUCTION

Cutting force analysis plays a vital role in studying the micro milling processes. The stress variation on the shaft of a micro-tool is much higher than that on a conventional tool, as in micro milling operations the feed per tooth to tool radius ratio has to be higher than in conventional milling to keep productivity at a reasonable level [1].

Due to the small size of the micro-tools, it is very difficult to notice the damage in the cutting edges and an inappropriate selection of the cutting conditions can cause the tool to brake unexpectedly. This paper investigates a thread making process in micro scale, called micro thread milling operation (MTMO) and presents a new model. The micro-tools used in this operation have a diameter of less than 2 mm.

Threading a workpiece is a fundamental metalworking process. Threads can be produced in a variety of ways, involving

two basic methods: plastic deformation working or metal cutting. The dominant method used in industry is plastic deformation working. Conventional bolts and screws, for example, are mostly made by this method. Threads produced by plastic deformation are stronger because of the grain structure than those produced by cutting, although forming cannot achieve the high accuracy and precision required in many applications. In thread milling high tool pressure are generated which can result into an excessive tool deflection and tool breakage when milling at full thread [2]. Threads made of brittle materials also cannot be produced by plastic deformation working. In such cases, thread cutting is necessary [3]. The common cutting processes for producing internal threads are tapping and thread milling. Tapping is used to make internal threads with the same diameter of the tool. It is done by feeding the cutting tool into the hole until the desired thread depth is achieved, then reversing the tap to back it out of the hole and remove it from the workpiece. Thread milling tools can produce internal threads with any diameter bigger than the tool diameter as well as external threads. In thread milling, the machine tool executes the thread in one single pass. The tool goes down to the hole and begins the cutting from the deepest part to the top in a helical path, or it begins at the top and goes until the end of the hole. Many authors developed models for prediction of forces in machining. These include analytical, experimental, mechanistic and numerical methods [4]. In thread cutting by tapping, a mechanistic method for the prediction of forces was presented by [5]. A number of papers describing the thread milling operation have been published [3] but there is no model to predict the forces involved in the process for micro thread cutting.

Bao and Tansel [1] proposed an analytical force model for micro end milling process based on Tlustý's model [7], but using a new expression for the chip thickness. They computed by the trajectory of the tool tip and observed that the model gives a good result at higher feed rate which supports his assumption that feed per tooth to tool radius is larger in micro end milling than in the conventional end milling operation. Zaman et al. [8] established a new concept to estimate the cutting force in micro



Figure 1. Micro Thread Cutting [6]

end milling by estimating the theoretical chip area instead of undeformed chip thickness.

The objective of this article is to present a mechanistic model for micro thread milling. The tool geometry analyzed involves triangular and metric threads with pitches until 0.45mm. The micro thread milling tool in this article has helical flutes and its geometry is analyzed as a modified micro end milling tool. Tool run out is added to the model and some examples of thread milling processes are presented and compared [9][10].

Nomenclature

d_e = external tool diameter, mm

d_i = internal tool diameter, mm

d_E = external workpiece diameter, mm

d_I = internal workpiece diameter, mm

d_h = hole diameter, mm

$d(z)$ = local diameter, mm

e = width of cut, mm

f_t = feed per tooth, mm

H = thread height, mm

K_n = normal specific cutting pressure, N/mm^2

K_f = radial specific cutting pressure, N/mm^2

K_z = axial specific cutting pressure, N/mm^2

N_f = number of flutes

p = thread pitch, mm

t_c = chip thickness, mm

V_c = cutting speed, m/min

Greek Symbols

α = rake angle, deg

δ = angle for the total engagement of a cutting edge, deg

ζ = angle between the flutes, deg

λ = helix angle, deg

ξ = thread angle, deg

φ_1 = initial angle of contact

φ_2 = final angle of contact

ϕ = angular position of a point in a flute

ψ = angular position of the leading point of the cutting edge

Subscripts

e - relative to external tool diameter

E - relative to external workpiece diameter

i - relative to internal tool diameter

I - relative to internal workpiece diameter

f, n, z - relative to the tool referential

x, y, z - relative to the workpiece referential

II. MICRO THREAD MILLING GEOMETRY

A. Tool Geometry

The threads studied in this article are metric and triangular. The thread variables presented in Fig. 2 are: thread pitch, p , thread angle, t , external workpiece diameter, d_E , internal workpiece diameter, d_I , and thread height H . The relation between the diameters can be written as [2][11]:

$$d_I = d_E - \frac{p}{\tan(\xi/2)} \quad (1)$$

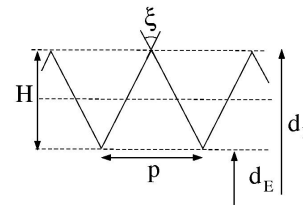


Figure 2. Thread geometry

The micro thread milling tool is very similar to an micro end milling tool. The tool geometry of a helical thread flute is presented in Fig. 3. The helix angle λ , the rake angle α (not shown in the figure), the internal and external diameters d_i and

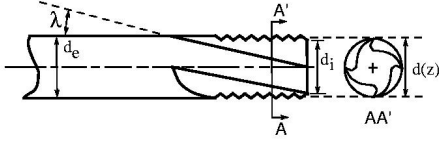


Figure 3. Thread Milling Tool Geometry

d_e and the number of flutes N_f define the tool geometry. The angle between the flutes is:

$$\xi = \frac{2\pi}{N_f} \quad (2)$$

and the number of each flute is n , $1 \leq n \leq N_f$. The local diameter $d(z)$ is written as a function of the height z , $d_i \leq d(z) \leq d_e$, calculated as follows:

$$d(z) = \begin{cases} d_i + \frac{2(z-nt(z)\frac{p}{2})}{\tan \xi/2}, & \text{if } nt(z) \text{ is odd} \\ d_i - \frac{2(z-nt(z)\frac{p}{2})}{\tan \xi/2}, & \text{if } nt(z) \text{ is even} \end{cases} \quad (3)$$

where $nt(z)$ is:

$$nt(z) = \text{IntegerPart} \frac{2z}{p} \quad (4)$$

The tool motion is circular in the plane normal to the tool-axis and linear in the direction of the tool-axis with a stationary workpiece to generate the thread. The workpiece is predrilled and the diameter of the hole is called d_h . The width of cut (or radial depth of cut) is $e(z)$:

$$e(z) = \frac{d(z) - d_h}{2} \quad (5)$$

B. Cutting Geometry

The cutting geometry of the micro thread milling process is different than the micro end milling because the cutting edge is not a straight line and the tool follows a circular trajectory. Following the approach used by [7] the contact interface in thread milling process can be described as shown in Fig. 4, where the depth of cut, b , can be observed.

The contact surface is divided in three phases: **A**, where the length of active cutting edge increases in time, **B**, where it is constant, and **C** where it decreases. There are two different types of contact surface geometry according to the relation between the angle δ , defined in Eq. (6), and the contact angle: *Type I* and *Type II*. It is a *Type I* geometry if $\delta \leq \varphi_2$, and *Type II* occurs if $\delta \geq \varphi_2 = \varphi_1$.

$$\delta = \frac{2b \tan \lambda}{d_e} \quad (6)$$

The contact angle is defined as the difference between the initial angle φ_1 and the final angle φ_2 . Two auxiliary angles were

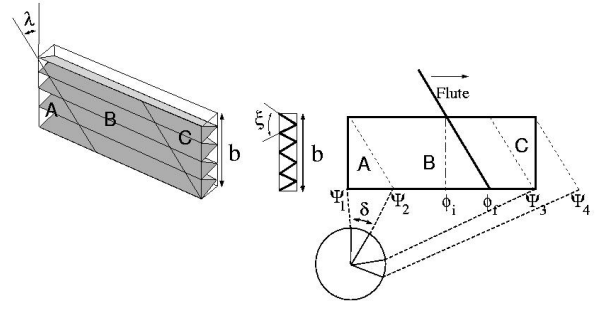


Figure 4. Contact phases

TABLE I. Limits of $\phi_i(\theta)$ and $\phi_f(\theta)$ in A, B and C [11]

Phase	Type I		Type II	
	$\phi_i(\theta)$	$\phi_f(\theta)$	$\phi_i(\theta)$	$\phi_f(\theta)$
For $\psi_1 \leq \theta \leq \psi_2$ - Phase A	φ_1	θ	φ_1	θ
For $\psi_2 \leq \theta \leq \psi_3$ - Phase B	$\theta - \delta$	θ	φ_1	φ_2
For $\psi_3 \leq \theta \leq \psi_4$ - Phase C	$\theta - \delta$	φ_2	$\theta - \delta$	φ_2

defined by [7] to analyze the flute movement through the three phases A, B and C. The first one is angle ψ , which indicates the angular position of the leading point of the cutting edge. The other one is angle ϕ , which indicates the position of the other points of the same flute. For a known ψ , the range of values for ϕ is between ϕ_i and ϕ_f , and it changes for each phase and each position θ of the tool as shown in Table I. The range of values for in each phase is shown on Table II and the limits of each phase are called ψ_1, ψ_2, ψ_3 and ψ_4 .

For a helical tool, the height z can be expressed as a function of the position of the tool θ and the point angle ϕ :

$$Z(\theta, \phi) = \frac{d_i(\theta - \phi)}{2 \tan \lambda} \quad (7)$$

In the case I, shown in Fig. 5, the tool feed velocity does not change direction, as occurs in end milling. In case II the tool cuts in a the circular path, Fig. 6.

C. Case I

For up milling the initial angle is zero. In case I the final angle is written as:

$$\varphi_2 = \frac{c \tan \lambda}{re} \quad (8)$$

TABLE II. Values of ψ_1, ψ_2, ψ_3 and ψ_4 for *Type I* and *Type II*.

	Type I	Type II
ψ_1	φ_1	φ_1
ψ_2	$\varphi_1 + \delta$	φ_2
ψ_3	φ_2	$\varphi_1 + \delta$
ψ_4	$\varphi_2 + \delta$	$\varphi_2 + \delta$

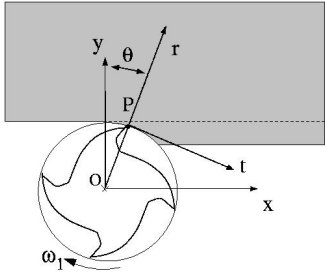


Figure 5. Linear tool path

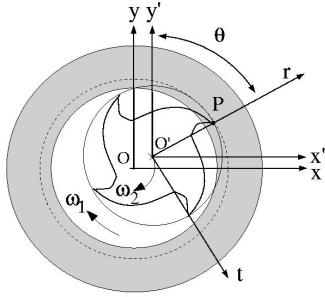


Figure 6. Circular tool path

D. Case II

In case II (Fig. 7), the final angle is written as:

$$\varphi_2 = \arcsin \frac{d_h^2 - d_i^2 - 4r_o}{4d_h r_o} \quad (9)$$

where $r_o = \frac{d_E - d_e}{2}$.

The uncut chip thickness for any point of the cutting edge, located in the height z and by the angle ϕ (Fig. 7), can be written as [1]:

$$t_c(\phi, n) = f_t \sin \phi - \frac{N_n}{\pi d(z)} f_t^2 \sin \phi \cos \phi + \frac{1}{d(z)} f_t^2 \cos^2 \phi \quad (10)$$

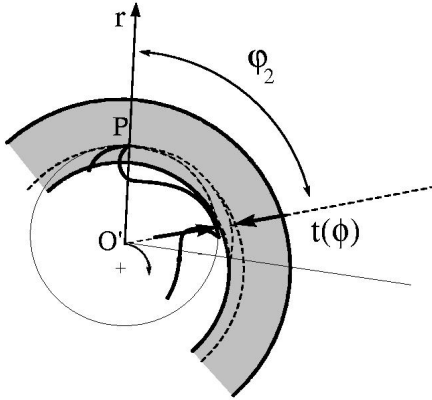


Figure 7. Chip thickness for case II

III. CHIP LOAD AREA MODEL

Elemental normal and frictional forces are required to the determination of cutting forces for a given geometry. The mechanistic modelling approach is a combination of analytical and empirical methods in which the forces are proportional to the chip load [12]. The specific cutting pressure, K_n , K_f and K_z , have been shown as a function of chip thickness t_c and cutting speed V_c [5].

$$\begin{aligned} F_n(\theta) &= K_n A(\theta) \\ F_f(\theta) &= K_f A(\theta) \\ F_z(\theta) &= K_z A(\theta) \end{aligned} \quad (11)$$

using a semi empirical modelling as [8], relating specific cutting pressures by an empiric factor:

$$\begin{aligned} F_n(\theta) &= K_n A(\theta) \\ F_f(\theta) &= m_1 K_n A(\theta) \\ F_z(\theta) &= m_2 K_n A(\theta) \end{aligned} \quad (12)$$

$$\ln K_n = a_0 + a_1 \ln(t_c) + a_2 \ln(t_c) + a_3 \ln(t_c) \ln(V_c) \quad (13)$$

The coefficients a_0 , a_1 , a_2 and a_3 are called specific cutting energy coefficients. They are dependent on the tool and workpiece materials and also on the cutting speed and the chip thickness. They are determined from calibration tests for a given tool workpiece combination and for a given range of cutting conditions.

A. Chip Cross Area

The function of chip cross area for the first flute $A_1(\theta)$ is:

$$A_1(\theta) = \int_{\phi_i(\theta)}^{\phi_f(\theta)} t(\phi, z) db \quad (14)$$

where db is [7]:

$$db = \frac{d(z)}{2 \tan \lambda} d\phi \quad (15)$$

Using Eq. 14 and 15, the area $A_1(\theta)$ can be calculated as:

$$A_1(\theta) = \int_{\phi_i(\theta)}^{\phi_f(\theta)} t(\phi, z(\theta, \phi)) \frac{d(z)}{2 \tan \lambda} d\phi \quad (16)$$

The limits $\phi_i(\theta)$ and $\phi_f(\theta)$ are functions of the and the cutting phase of θ , as shown in Table I. In order to add the contributions of all flutes, the chip cross-sectional area function for each flute (n) is written as:

$$A_n(\theta) = \int_{\phi_i(\theta + \zeta(n-1))}^{\phi_f(\theta + \zeta(n-1))} t(\phi, z(\theta, \phi)) \frac{d(z)}{2 \tan \lambda} d\phi \quad (17)$$

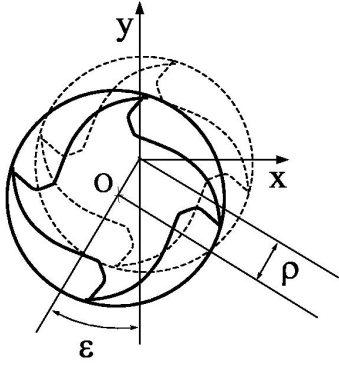


Figure 8. Tool run out [13]

In Eq. 17 ϕ_1 and ϕ_2 are also written as a function of n . The total area $A(\theta)$ is calculated as:

$$A(\theta) = \sum_{n=1}^{N_f} A_n(\theta) \quad (18)$$

B. Tool Run Out

Cutter run out exists in all kinds of milling operations and results in variations in the undeformed chip thickness, local forces and machined surface characteristics. The run out can be due to cutter axis offset, eccentricity (ρ) or cutting points positioning offset (ϵ), shown in Fig. 8, and it depends principally on the characteristics of the spindle and tool holder. The chip thickness for milling in presence of run out was rewritten by [13] and adapted for micro milling by [14]. Using Bao equation for run-out for thread micro milling, $d(z)$ should be included:

$$\begin{aligned} t_c(\theta, \phi, n) = & f_t \left[1 + (-1)^n \frac{\rho}{\pi d(z(\theta, \phi))} \sin \epsilon \right] \sin \phi \\ & - \frac{1}{2\pi d(z)} f_t^2 \sin \phi \cos \phi \\ & + \frac{1}{d(z(\theta, \phi))} f_t^2 \cos^2 \phi - (-1)^2 2\rho \cos \epsilon \end{aligned} \quad (19)$$

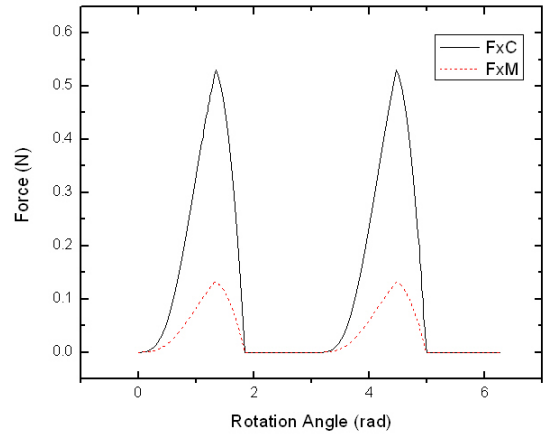
IV. NUMERICAL RESULTS

In order to analyze the forces profile in thread milling, four examples are presented in this article, the commercial upper and lower geometric limits for micro thread milling tool with and without runout. Specific pressure in these examples will be the same taken from [8] by $K_f = 13.5 \text{ MPa}$, $m_1 = 8$ and $m_2 = 4$ (proposed here). The geometry of cut and the velocities are: $\omega = 10000 \text{ rpm}$, $f = 150 \text{ mm/min}$.

A. Tool 1

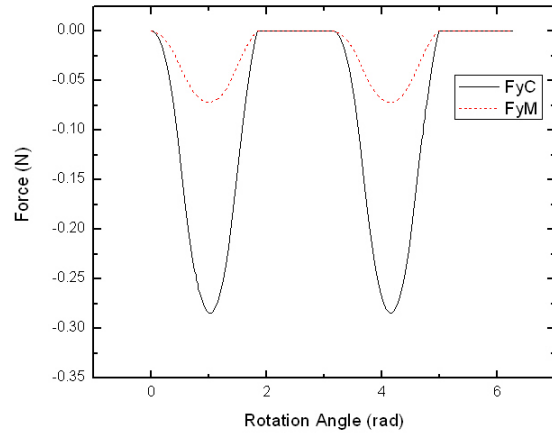
The tool 1 is used in the simulations 1a and 1b and has the following parameters: $d_e = 1 \text{ mm}$, $p = 0.25 \text{ mm}$, $\lambda = 30 \text{ deg}$, $N_f = 2$ and $\xi = 60 \text{ deg}$. Figure 9 compares the thread milling

M1 - Thread Cutting Modeling (Conventional Model and Micro Model)



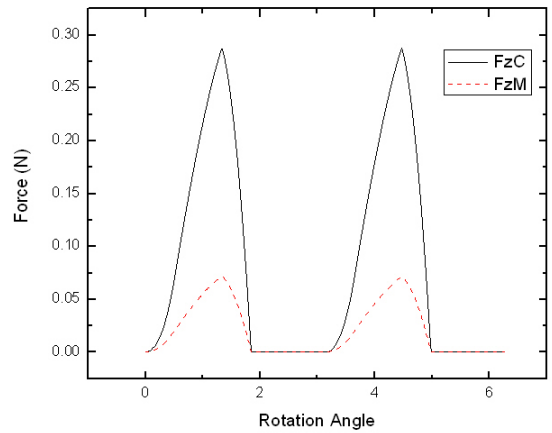
(a) Fx

M1 - Thread Cutting Modeling (Conventional Model and Micro Model)



(b) Fy

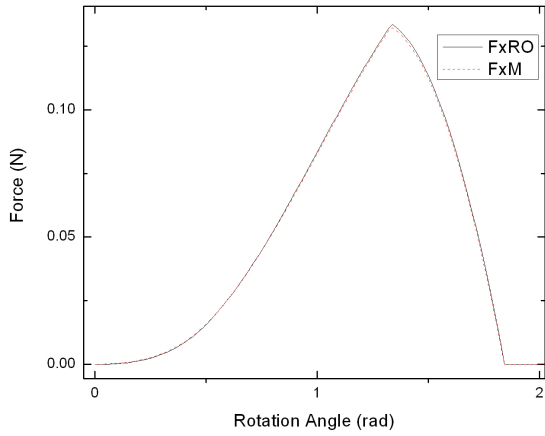
M1 - Thread Cutting Modeling (Conventional Model and Micro Model)



(c) Fz

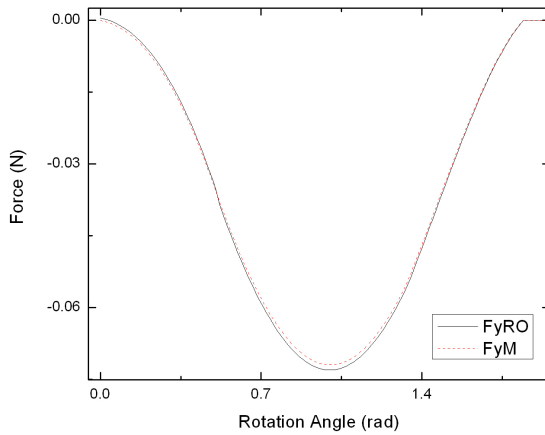
Figure 9. Thread Cutting Model for M1 - Simulation 1a

M1 - Thread Cutting Modeling (Micro Model with and without RunOut)



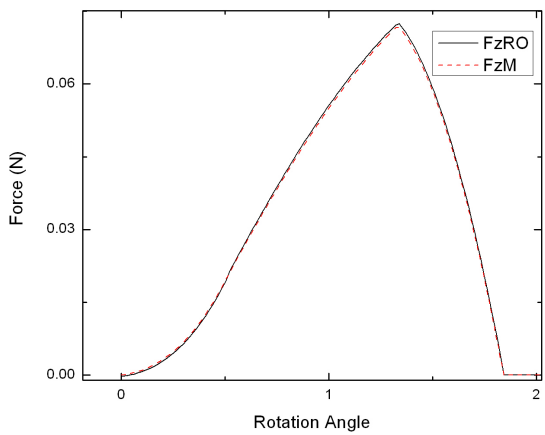
(a) Fx

M1 - Thread Cutting Modeling (Micro Model with and without RunOut)



(b) Fy

M1 - Thread Cutting Modeling (Micro Model with and without RunOut)



(c) Fz

Figure 10. Thread Cutting Model for M1 with and without run-out - Simulation 1b

force for M1 tool using conventional model (CTMO) and named in the figure as F_{xC} , F_{yC} and F_{zC} with forces calculated with micro thread milling model based on Bao [1] micro chip thickness (named in figure as F_{xM} , F_{yM} and F_{zM}).

Figure 10 compares the micro thread milling model based on Bao [1] micro chip thickness (named in figure as F_{xM} , F_{yM} and F_{zM}) with and without the run-out (F_{xRO} , F_{yRO} and F_{zRO}). The run-out parameters used were $\rho = 0.1mm$ and 10° .

B. Tool 2

The tool 2 is used in simulations 2a and 2b and has the following parameters: $d_e = 2.5mm$, $p = 0.45mm$, $\lambda = 30^\circ$, $N_f = 2$ and $\xi = 60^\circ$. Figure 11 compares the thread milling force for M2.5 tool using conventional model (CTMO) and named in the figure as F_{xC} , F_{yC} and F_{zC} with forces calculated with micro thread milling model based on Bao [1] micro chip thickness (named in figure as F_{xM} , F_{yM} and F_{zM}).

Figure 12 compares the micro thread milling model based on Bao [1] micro chip thickness (named in figure as F_{xM} , F_{yM} and F_{zM}) with and without the run-out (F_{xRO} , F_{yRO} and F_{zRO}). The run-out parameters used were $\rho = 0.1mm$ and 10° .

V. CONCLUSIONS

A mechanistic model have been adapted for micro thread milling. The model takes into account the thread cutting edge and the linear movement of the tool and the chip thickness calculated for micro milling processes. The forces were predicted for two different tools with two condition: without tool run-out and with a 0.1mm run-out, that for micro milling is very high. Even thought, comparing forces considering and disregarding run-out, the differences could be neglected. The results show that comparing tool forces for micro thread milling using Martellotti model or using Bao model the first one over estimates in more than twice on the amplitude. The model should be compared with experimental data and the model can include the circular tool path as in [15] and [16].

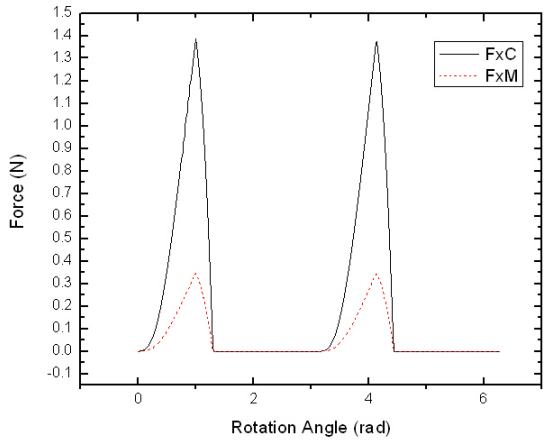
ACKNOWLEDGMENT

The authors acknowledge the support of the Brazilian Research Councils CNPq and FAPERJ.

REFERENCES

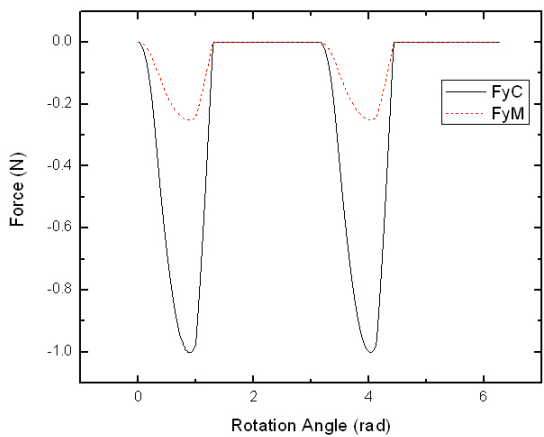
- [1] W. Y. Bao and I. N. Tansel, "Modeling micro-end-milling operations. part i: analytical cutting force model," *International Journal of Machine Tools and Manufacture*, vol. 40 (15), 2000, pp. 2155 – 2173.
- [2] A. C. Araujo, J. L. Silveira, M. B. Jun, S. G. Kapoor, and R. DeVor, "A model for thread milling cutting forces," *International Journal of Machine Tools and Manufacture*, vol. 46 (15), 2006, pp. 2057 – 2065.
- [3] S. Smith and J. Tlusty, "An overview of modeling and simulation of the milling process," *Journal of Engineering for Industry*, vol. 113, 1991, pp. 169–175.

M2.5 - Thread Cutting Modeling (Conventional Model and Micro Model)



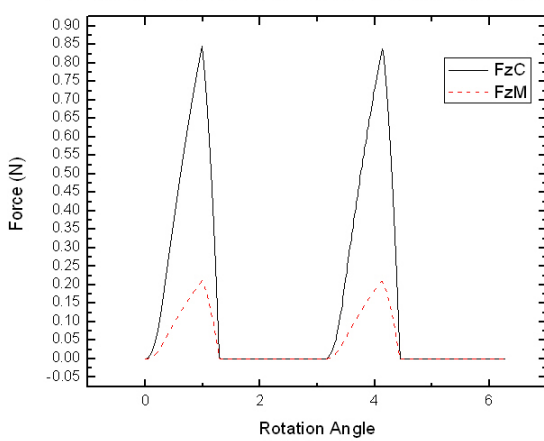
(a) Fx

M2.5 - Thread Cutting Modeling (Conventional Model and Micro Model)



(b) Fy

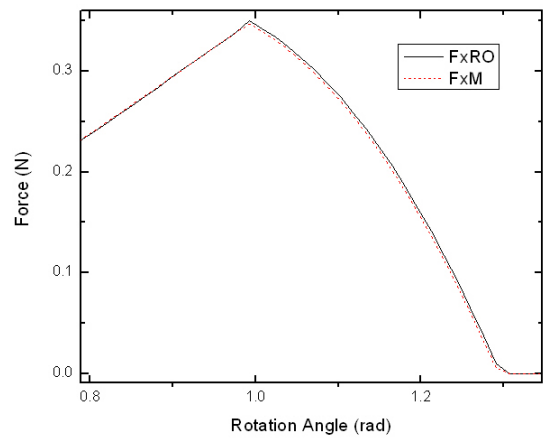
M2.5 - Thread Cutting Modeling (Conventional Model and Micro Model)



(c) Fz

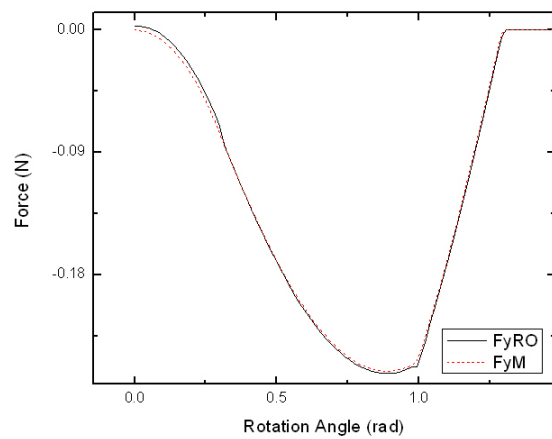
Figure 11. Thread Cutting Model for M25 - Simulation 2a

M2.5 - Thread Cutting Modeling (Micro Model with and without RunOut)



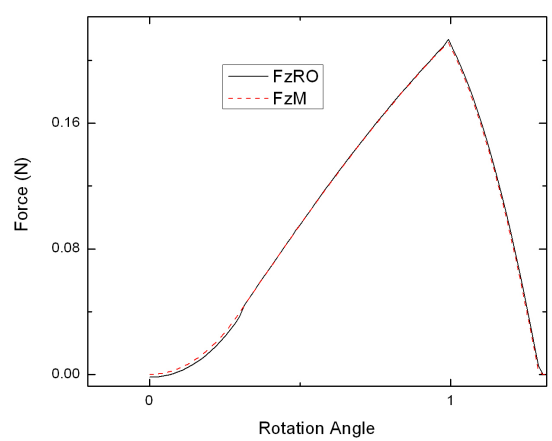
(a) Fx

M2.5 - Thread Cutting Modeling (Micro Model with and without RunOut)



(b) Fy

M2.5 - Thread Cutting Modeling (Micro Model with and without RunOut)



(c) Fz

Figure 12. Thread Cutting Model for M25 with and without run-out - Simulation 1b

- [4] K. F. Ehmann, S. G. Kapoor, R. E. DeVor, and I. Lazoglu, "Machining process modeling: a review," *Journal of Manufacturing Science and Engineering, Transactions of the ASME*, vol. 119, 1997.
- [5] A. P. S. Dogra, S. G. Kapoor, and R. E. DeVor, "Mechanistic model for tapping process with emphasis on process faults and hole geometry," *Journal of Manufacturing Science and Engineering, Transactions of the ASME*, vol. 124 (1), 2002, pp. pp. 18–25.
- [6] K. group, "Komet jel mgf xh micro m1-m2.5," website, April 2010.
- [7] J. Tlustý and J. MacNeil, "Dynamics of cutting in end milling," *Annals of CIRP*, vol. 24 (1), 1975, pp. pp. 213–221.
- [8] M. Zaman, A. S. Kumar, M. Rahman, and S. Sreeram, "A three-dimensional analytical cutting force model for micro end milling operation," *International Journal of Machine Tools and Manufacture*, vol. 46 (3-4), 2006, pp. 353 – 366.
- [9] I. Kang, J. Kim, J. Kim, M. Kang, and Y. Seo, "A mechanistic model of cutting force in the micro end milling process," *Journal of Materials Processing Technology*, vol. 187-188, 2007, pp. 250 – 255, 3rd International Conference on Advanced Forming and Die Manufacturing Technology.
- [10] G. Newby, S. Venkatachalam, and S. Liang, "Empirical analysis of cutting force constants in micro-end-milling operations," *Journal of Materials Processing Technology*, vol. 192-193, 2007, pp. 41 – 47, the Seventh Asia Pacific Conference on Materials Processing (7th APCMP 2006).
- [11] A. C. Araujo, J. L. Silveira, and S. G. Kapoor, "Force prediction in thread milling," *Journal of the Brazilian Society of Mechanical Sciences and Engineering*, vol. 1 (XXVI), 2004, pp. pp. 82–88.
- [12] W. Kline, R. DeVor, and J. Lindberg, "The prediction of cutting forces in end milling with application to cornering cuts," *International Journal of Machine Tool Design and Research*, vol. 22 (1), 1982, pp. 7 – 22.
- [13] W. Kline and R. DeVor, "The effect of runout on cutting geometry and forces in end milling," *International Journal of Machine Tool Design and Research*, vol. 23 (2-3), 1983, pp. 123 – 140.
- [14] W. Y. Bao and I. N. Tansel, "Modeling micro-end-milling operations. part ii: tool run-out," *International Journal of Machine Tools and Manufacture*, vol. 40 (15), 2000, pp. 2175 – 2192.
- [15] M. B. G. Jun and A. C. Araujo, "Modeling and analysis of the thread milling operation in the combined drilling/thread milling process," *ASME Conf. Proc. MSEC2008*, vol. 1, 2008.
- [16] M. B. G. Jun and A. C. Araujo, "Modeling of the thread milling operation in a combined thread/drilling operation: Thrilling," *J. Manuf. Sci. Eng.*, vol. 132, 2010.